THE EFFECT OF OBJECT POTENTIALS ON THE WAKE OF A
FLOWING PLASMA(U) S-CUBED LA JOLLA CA   I. KATZ ET AL.
DEC 86 SSS-R-87-8473 AFGL-TR-87-0023 F19620-86-C-0056

1/1

F/G 20/9   NL

END
/0 87
DTIC

1.0 2.8 2.5

1.1 3.2 2.2

3.6 2.0

1.8

1.25 1.4 1.6

MICROCOPY RESOLUTION TEST CHART

AD-A184 038

⑫

AFGL-TR-87-0023

The Effect of Object Potentials on the Wake of a Flowing Plasma

I. Katz
M. J. Mandell
D. E. Parks
K. Wright
N. H. Stone
U. Samir

DTIC
S ELECTE D
SEP 0 3 1987
C D

S-CUBED
A Division of Maxwell Laboratories
P.O. Box 1620
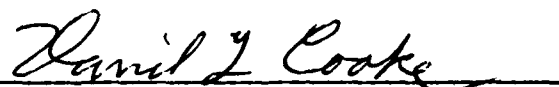La Jolla, CA 92038

December 1986

Scientific Report No. 3

87 9 2 009

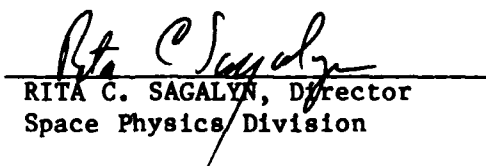"This technical report has been reviewed and is approved for publication"

DAVID COOKE
Contract Manager
Spacecraft Interactions Branch
  Space Physics Division

CHARLES P. PIKE, Chief
Spacecraft Interactions Branch
Space Physics Division

FOR THE COMMANDER

RITA C. SAGALYN, Director
Space Physics Division

This report has been reviewed by the ESD Public Affairs Office (PA) and is releasable to the National Technical Information Service (NTIS).

Qualified requestors may obtain additional copies from the Defense Technical Information Center. All others should apply to the National Technical Information Service.

If your address has changed, or if you wish to be removed from the mailing list, or if the addressee is no longer employed by your organization, please notify AFGL/DAA, Hanscom AFB, MA 01731. This will assist us in maintaining a current mailing list.

Do not return copies of this report unless contractual obligations or notices on a specific document requires that it be returned.

AD-A184 038

REPORT DOCUMENTATION PAGE

1a. REPORT SECURITY CLASSIFICATION UNCLASSIFIED		1b. RESTRICTIVE MARKINGS None			
2a. SECURITY CLASSIFICATION AUTHORITY None		3. DISTRIBUTION / AVAILABILITY OF REPORT Approved for public release; distribution unlimited.			
2b. DECLASSIFICATION / DOWNGRADING SCHEDULE Immediate					
4. PERFORMING ORGANIZATION REPORT NUMBER(S) SSS-R-87-8473		5. MONITORING ORGANIZATION REPORT NUMBER(S) AFGL-TR-87-0023			
6a. NAME OF PERFORMING ORGANIZATION S-CUBED, A Division of Maxwell Laboratories	6b. OFFICE SYMBOL (If applicable)	7a. NAME OF MONITORING ORGANIZATION Air Force Geophysics Laboratory			
6c. ADDRESS (City, State, and ZIP Code) P.O. Box 1620 La Jolla, CA 92038		7b. ADDRESS (City, State, and ZIP Code) Hanscom Air Force Base Massachusetts 01731			
8a. NAME OF FUNDING / SPONSORING ORGANIZATION Air Force Geo- physics Laboratory (AFGL/PHK)	8b. OFFICE SYMBOL (If applicable)	9. PROCUREMENT INSTRUMENT IDENTIFICATION NUMBER Contract F19628-86-C-0056			
8c. ADDRESS (City, State, and ZIP Code) Hanscom Air Force Base, MA 01731		10. SOURCE OF FUNDING NUMBERS			
		PROGRAM ELEMENT NO. 62101F	PROJECT NO. 7601	TASK NO. 30	WORK UNIT ACCESSION NO. AA

11. TITLE *(Include Security Classification)*

The Effect of Object Potentials on the Wake of a Flowing Plasma

12. PERSONAL AUTHOR(S)
I. Katz, M. J. Mandell, D. E. Parks, K. Wright, N. H. Stone, U. Samir

13a. TYPE OF REPORT Scientific Report No. 3	13b. TIME COVERED FROM_____ TO_____	14. DATE OF REPORT (Year, Month, Day) December 1986	15. PAGE COUNT 32

16. SUPPLEMENTARY NOTATION

17	COSATI CODES		18. SUBJECT TERMS *(Continue on reverse if necessary and identify by block number)*
FIELD	GROUP	SUB-GROUP	Plasma Wake, Spacecraft Wake, Mesosonic Flow

19. ABSTRACT *(Continue on reverse if necessary and identify by block number)*

Measurements and calculations have been carried out to determine the structure of electric potential and ion density in the near wake created by the flow of a high Mach number plasma past a conducting plate biased with respect to the undisturbed plasma. Results are obtained for a molecular nitrogen plasma with ambient electron densities N of order 10^5 cm^{-3}, ion temperatures $\theta_i \approx 0.025$eV, electron temperatures $\theta \sim 0.3$eV, and plasma flow velocities $V_0 \approx 10^6$ cm/sec, corresponding to $V_0/(\theta/M)^{1/2} \approx 11$.

For high Mach number flow past an unbiased object, the wake structure is very nearly that predicted for the expansion of an initially uniform plasma half space into vacuum; in this case there is a sharply defined ion front moving under the influence of an electric field produced by charge separation between ions and electrons near the front.

(Continued over)

20. DISTRIBUTION / AVAILABILITY OF ABSTRACT ■ UNCLASSIFIED/UNLIMITED ☐ SAME AS RPT. ☐ DTIC USERS	21. ABSTRACT SECURITY CLASSIFICATION UNCLASSIFIED	
22a. NAME OF RESPONSIBLE INDIVIDUAL David L. Cooke	22b. TELEPHONE (Include Area Code)	22c. OFFICE SYMBOL AFGL/PHK

DD FORM 1473, 84 MAR   83 APR edition may be used until exhausted.
All other editions are obsolete.

19. Abstract (continued)

With bias potential ϕp such that $q\phi p/\theta$ is in the range -1 to -10, a well defined ion front still exists, but its motion is strongly affected by the imposed potential. This effect can be explained in terms of the impulse received by those ions passing through the sheath region near the plate edge.

Two-dimensional simulations of the laboratory experiments were performed using a multiple waterbag technique. The results for both zero and finite ion temperatures are almost noise free, and support the approximate analytical model. The calculated density for 10 θ negative bias on the plate is compared with the measured profile.

Nomenclature

e	– Mathematical constant 2.71828
E, E_o, E_i, E_{oo}	– Electric fields (see text)
M	– Ion mass
N	– Ambient plasma density
n	– Local ion density
n_e	– Local electron density
q	– Magnitude of electron charge
R	– Range of perturbing field
t	– Time coordinate
u	– Coordinate locally parallel to ion trajectory
v	– Local ion speed
V_o	– Ion flow speed
V_x	– Transverse component of ion velocity
w	– Coordinate locally normal to ion trajectory
x	– Coordinate normal to ion flow
x_F	– Position of ion front measured 22.4 cm downstream
z	– Coordinate parallel to ion flow
a	– Free parameter
ϵ_o	– Permittivity of free space
θ	– Electron temperature
θ_i	– Ion temperature (transverse motion)
λ_D	– Debye length
ϕ	– Electrostatic potential
ϕ_p	– Applied potential on metal plate
ω	– Ion plasma frequency

1. Introduction

A number of authors have reviewed the structure of the wake generated by relative motion between an object and a collisionless plasma.[1-5] These reviews have considered the wake structure extending from the near wake to the far wake for various ranges of body size R_o relative to the ambient plasma Debye length λ_D and for various conditions of electrical potential on the body relative to the ambient plasma.

This study focuses on the structure of the ion front in the near wake behind a semi-infinite plate, and in particular on the effect of plate potential on the structure of the ion front. The present analysis, which is relevant to the wake structure of a large body traversing the ionosphere, is motivated by the experiments on wakes performed in a large vacuum tank[6]. Fig. 1 depicts the experimental situation. The measured results obtained by means of a differential ion flux probe consist of ion density profiles as a function of x at a given downstream position. The plate is biased to a potential ϕ_p relative to the tank wall, and ϕ_p may differ from the potential ϕ_a of the plasma in the neighborhood of the plate. The effect of ϕ_p (or $\phi_p-\phi_a$) on the motion and structure of the ion front in the wake behind the plate is determined.

The analysis, exploiting the approximate relationship between the problems of a mesosonic wake and the expansion of plasma into vacuum

1

considers first the effect of an applied electric field on the initial plasma expansion. Specific calculations of wake structure, including the effect of an applied potential and of ion temperature, are given and compared with experiment in Section 3.

2. Effect of Potential on Expansion into Vacuum

For zero bias, the electric field at the ion front $x_F(z)$ is given approximately by[7]

$$\frac{qE}{M} = 2\sqrt{\frac{\theta}{M}} \frac{\alpha w}{1 + \alpha w t} \left\{ 1 - \left[1 - \left(\frac{2e}{\alpha} \right)^{1/2} \right] \frac{1}{1 + \alpha w t} \right\}$$ (1)

$$t = z/V_o$$

with the adjustable parameter α, $e = 2.718$, and ions travel with velocity V_o in the positive Z direction. Here q and M are the ion charge and mass, respectively, θ the electron temperature and

$w = \left[\frac{Nq^2}{\epsilon_o M} \right]^{1/2}$ the ion plasma frequency for ambient density N. The semi-empirical formula (1) was constructed to reproduce, independent of α, certain theoretically known properties of expansion of a plasma half space into vacuum, namely the asymptotic dependence of the ion front on t for $wt \gg 1$[8], and the value of E at $t = 0$, namely $E_o = (2N\theta/\epsilon_o e)^{1/2}$.[9] The position and velocity of the front calculated from eq. (1) are in good agreement with the measurements of Wright, Stone and Samir.[6]

2

Let us now consider how the expansion into vacuum is modified by an applied field E_i in the vacuum region. Initially the ion density is N (uniform) for $x < 0$, and zero for $x > 0$. The potential is determined from

$$-\epsilon_o \nabla^2 \phi = Nq \left[1-\exp\left(\frac{q\phi}{\theta}\right)\right] \quad x < 0$$
$$= Nq \, \exp\left(\frac{q\phi}{\theta}\right) \qquad x > 0 \tag{2}$$

and satisfies the conditions $\phi(x=-\infty) = 0$, $\phi(x=\infty) = -\infty$, $E(x=-\infty) = 0$, $E(x=\infty) = E_i$. The first integral of (2) over the plasma half space from $x = -\infty$ to $x=0$ yields

$$\frac{\epsilon_o}{2} E_o^2 = N\theta[\exp(q\phi_o/\theta) - 1 - q\,\phi_o/\theta] \tag{3}$$

where a subscript o denotes the value at the plasma vacuum interface. Integration over the vacuum region yields

$$\frac{\epsilon_o}{2} (E_o^2 - E_i^2) = N\theta \, \exp(q\phi_o/\theta) \tag{4}$$

For $E_i = 0$, $\phi_o = \phi_{oo}$ and $E_o = E_{oo}$ where

$$\frac{q\phi_{oo}}{\theta} = -1 \tag{5}$$

$$\frac{\epsilon_o}{2} E_{oo}^2 = N\theta e^{-1} \tag{6}$$

are the results obtained by Crow, Auer and Allen[9].

For $E_i \neq 0$,

$$- \frac{\epsilon_o}{2} E_i{}^2 = N\theta \left[1 + \frac{q\phi_o}{\theta} \right] \tag{7}$$

$$\frac{1}{2} E_o{}^2 = \frac{1}{2} E_i{}^2 + \frac{1}{2} E_{oo}{}^2 \, e^{- \frac{\epsilon_o E_i{}^2}{2N\theta}} \tag{8}$$

The applied field is the dominant component of the initial field if $\epsilon_o E_i{}^2 / 2N\theta > 1$. The applied field is, of course, a nebulous quantity; in particular, it is not unambiguously related to the value of the bias potential on an object over which a plasma is flowing. In order of magnitude however, E_i should be comparable to that of the sheath electric field which deflects the streaming ions before they enter the near wake downstream from the object; $E_i \sim \phi_o/R$ where ϕ_o is the potential on the object relative to that in the remote upstream plasma and R is a length scale for potential variation within the sheath. Rather than attempting to further pursue the analogy between the plasma expansion and the wake problems, we turn now to consideration of the two dimensional steady wake.

3. <u>Qualitative Effect of Potential on a Two-Dimensional Steady State Wake</u>

The expansion of a semi-infinite plasma into vacuum corresponds only approximately to the wake problem. In particular, the free expansion analogue does not take into account the fixed potential on the wake-forming plate, nor does it clearly suggest how to account for variations

4

in plate potential. A complete theory would be based on the steady state solutions of the Poisson and ion trajectory equations in at least two dimensions.

A primary effect neglected in the free expansion model is the transverse acceleration experienced by ions that pass from upstream ($z < 0$) through the sheath surrounding the tip of the plate before entering the wake region ($z > 0$, $x > 0$) (see Fig. 1). The sheath should extend in the upstream direction no more than a few λ_D, for $\phi_p \lesssim 10\theta$. In these circumstances the approximate effect of the sheath on fast ions ($1/2\, MV_o^2 \gg \phi_p$) can be described in terms of an impulsive change in transverse velocity, V_x:

$$M\, \Delta V_x \simeq qE\Delta t \qquad (9)$$

$$\simeq \frac{|q\, \phi_p|}{R}\, \frac{R}{V_o}$$

where R is the range of the force, i.e.

$$\frac{\Delta V_x}{V_o} \simeq \frac{q\phi_p}{M\, V_o^2} \qquad (10)$$

For the following parameters, corresponding to conditions in Wright's experiments[6]

$$\phi_p = -3 \text{ volts}$$

$$\frac{1}{2}\, MV_o^2 = 18 \text{ volts } (N_2^+)$$

5

$$\frac{\Delta V_x}{V_o} \simeq \frac{1}{12}$$

At a point $z = 22.4$ cm downstream, Δx (est) $= \frac{z}{V_o} \Delta V_x \sim 2$ cm.

Assuming that the effect of the finite plate potential on the wake is to deliver impulse to the ions, this means that the position x_F of the ion front will have shifted by an amount Δx relative to that for an unbiased plate. The shift in experimental values of x_F between $\phi_p = 0$ and $\phi_p = -3$ volts is

$$\Delta x \text{ (exp)} = .65 \text{ cm}.$$

Although of the right order of magnitude, the estimated Δx (est.) is 3 times Δx (obs) even before taking account of the effect of potential in the downstream direction. In any case, the impulse approximation given here leads to a displacement linear in applied potential, a conclusion not inconsistent with experimental results, at least for negative potentials.

For positive potentials, the effect of potential appears to be smaller than for negative potentials, except for an abrupt change between $\phi = 0$ and $\phi = +1$ volt. A smaller effect could be expected on the grounds that in the neighborhood of the plate the plasma will be only a few θ below ϕ_p for $\phi_p > 0$.

3. Two-Dimensional Calculations of Near Wake Structure

The experiment was simulated numerically in two dimensions using a finite element computer code. The code solves the Poisson-Vlasov equations in steady state. Potentials, ion trajectories, and ion densities were calculated self-consistently on the finite element mesh shown in Figure 2. The boundary conditions were zero potential at the top (ambient plasma) and left (input) boundaries, specified (imposed bias) potential on the metal plate, zero normal component of electric field on the right (exit) boundary, and $E_\perp = 2 \exp(\phi/\theta)$ on the lower (vacuum) boundary. For the finite element potential solution, the potential was assumed to vary bilinearly in each element. For calculating trajectories, however, a quadratic form was used to interpolate in the direction approximately normal to the ion front. This was necessary because the discontinuous electric fields obtained from linear interpolation caused bunching of ion trajectories, resulting in striations in the downstream ion density.

The ion density was calculated using a variant of the "waterbag" method[10,11]. This method takes advantage of the fact that, if trajectories do not cross, the current contained between two trajectory paths (in two dimensions, or in a "flux tube" in three dimensions) is constant. Denoting by u the dimension along the trajectories and by w the dimension normal to the trajectories, we have

$$I\Delta t = nv\Delta w\Delta t = n\Delta w\Delta u$$

where n and v are the local ion density and velocity. It follows that the density ratio for quadrilaterals formed by adjacent time points on adjacent trajectories (Figure 3) is the inverse ratio of their areas. Calculations were performed with initial (left boundary of grid) values of 0.1 and 0.2 Debye lengths for Δw and Δu respectively, with constant timesteps Δt. For the finite temperature case, the ions were divided into ten subspecies, each representing a different value of transverse velocity, and the resultant subspecies densities were added together. This technique for calculating ion densities resulted in very little numerical noise and no code diffusion, and proved far superior to particle-in-cell methods for cases such as this where a sharp ion density boundary exists.

The electron density was assumed to satisfy the "barometric law"

$$n_e/N = \exp(q\phi/\theta)$$

for negative potentials, and

$$n_e/N = 1 + q\phi/\theta$$

for positive potentials, where N and θ are the ambient plasma density $(10^{-5} \text{ cm}^{-3})$ and electron temperature (0.27 eV), and ϕ is the local

8

potential. Ion densities and potentials were iterated until neither changed more than one percent.

Figure 4 shows the electrostatic potentials calculated for the zero temperature, zero bias case. There are no electric fields seen upstream of the plate. Downstream, beyond a transition region of about one Debye length, the equipotential lines are nearly parallel to the ion flow direction, and equivalence to the one-dimensional time-dependent problem[9] is nearly exact. (Note that the influence of the plate extends several Debye lengths into the vacuum region.) Electrostatic potential for the case of the plate biased to -10θ is shown in Figure 5. In this case, the ions see very strong downward fields as they pass over the plate, providing the impulse described in Equation (10). Moreover, the influence of the plate potential is strongly felt by the ions for about ten Debye lengths downstream, providing additional downward force on the ion front.

Ion density profiles calculated 15 Debye lengths downstream of the plate are shown in Figure 6 for cold ions, and in Figure 7 for a transverse ion temperature, θ_i of 0.096 θ (300 degrees Kelvin). The two curves in each figure are for plate potentials of zero and -10 θ. The increase in front motion, (about 1.8 Debye lengths), corresponds closely with the 2 cm obtained from Equation (10). The finite temperature profiles are monotonic and considerably broader than the cold ion profiles. The angular spread of the ion front is a few times $(2\theta_i/MV_o^2)$, as expected. The only non-monotonic behavior is for cold

ions with zero potential on the plate. Figure 8(a-d) show the calculated densities throughout the region for the four cases.

The calculated finite temperature ion density is compared with the laboratory measurement in Figure 9. The general front amplitude and motion agrees well with experiment. However, the calculation has a broader front, while the experiment evidences an overshoot and undershoot.

4. Discussion

The calculated and experimental results show that wake closure is well described by the acceleration of ions in the plasma steady-state electric field. However, the electrostatic influence of the object creating the wake leads to significant differences between wake closure and the expansion of a plasma into vacuum.

For zero ion temperature and zero bias on the plate, the calculated front position $(0.50\lambda_D)$ is less than theoretically predicted $(0.72\lambda_D)$. This is due to the reduction of the transverse electric field at the front by the influence of the conducting plate for several λ_D downstream. The experimentally measured front position $(1.5\lambda_D)$ is appreciably greater than predicted.

The application of -10θ bias to the plate dramatically changes the electrostatic potential structure. The shift in front position

predicted by the crude "impulse" theory $(1.1\lambda_D)$ is in qualitative agreement with calculation $(1.8\lambda_D)$. The experimental shift $(0.5\lambda_D)$ is smaller, but the resultant front positions $(2\lambda_D$ experiment; $2.3\lambda_D$ calculation) agree well. Experiment and calculation also show excellent agreement as to the magnitude of density change at the ion front.

The calculations produce the expected thermal spread in the front. The experimental thermal spread is far less, suggesting that the transverse ion temperature is well below 300K. (Had we shown the zero temperature calculation on Figure 9, apparent agreement would have been near perfect.) However, an ion temperature of 300K produces no observable change (relative to zero temperature ions) in the electrostatic potential. We believe that the reason for lack of thermal spread in the experimental wake-front is that the ions originate from a small source, so that they are already "velocity-selected" when they enter the wake region.

Expansion of plasma into vacuum is a good approximate model for filling in a plasma wake. However, multi-dimensional effects due to the influence of the body creating the wake on the electrostatic potential structure cause noticeable departures from this model when the body is at plasma potential, and substantial departures when the body departs from plasma potential.

Acknowledgements

11

REFERENCES

1. Ya. L. Al'pert, A. V. Gurevich and L. P. Pitzaevskii, <u>Space Physics with Artificial Satellites</u>. (Plenum Press, New York, 1965)

2. V. C. Liu, "Ionospheric Gas Dynamics of Satellites and Diagnostic Probes," <u>Space Sci. Rev.</u>, <u>9</u>, 423, (1969).

3. A. V. Gurevich, L. P. Pitaevskii, and V. V. Smirnova, "Ionospheric Aerodynamics," <u>Space Sci. Rev.</u>, <u>9</u>, 805, (1969).

4. V. C. Liu, "On Ionospheric Aerodynamics," <u>Prog. Aerospace Sci.</u>, <u>16</u>, 273, (1975).

5. N. H. Stone, "The Aerodynamics of Bodies in a Rarefied Ionized Gas with Applications to Spacecraft Environmental Dynamics," NASA Technical Paper 1933, (1981).

6. K. H. Wright, Jr., N. H. Stone, and U. Samir, "A Study of Plasma Expansion Phenomena in Laboratory Generated Plasma Wakes: Preliminary Results," <u>J. Plasma Phys.</u>, <u>33</u>, 71, (1985).

7. I. Katz, D. E. Parks and K. H. Wright, Jr., "A Model of the Plasma Wake Generated by a Large Object," <u>IEEE Trans. Nucl. Sci., Vol. NS-32</u> (6), 4092, (1985).

8. A. V. Gurevich and A. P. Mashcherkin, "Ion Acceleration in an Expanding Plasma," <u>Sov. Phys. JETP</u>, <u>53</u>, 937, (1981).

9. J. E. Crow, P. J. Auer, and J. E. Allen, "The Expansion of a Plasma into Vacuum," <u>J. Plasma Phys.</u>, <u>14</u>, 65, (1975).

10. H. L. Berk, C. E. Nielsen, and K. V. Roberts, <u>Phys. Fluids</u>, <u>13</u>, 980 (1970).

11. A. C. Calder and J. G. Laframboise, "Multiple-Water-Bag Simulation of Inhomogeneous Plasma Motion near an Electrode," <u>Journal of Computational Physics</u>, <u>65</u>, 18 (1986).

FIGURES

Figure 1.   Schematic illustration of experiment to measure ion density in wake behind a biased plate.

Figure 2.   Finite element mesh used to calculate potentials and ion trajectories in the wake behind a biased plate. (Distances are in Debye lengths.)

Figure 3.   Schematic of method for determining ion densities. Quadrilaterals are drawn between adjacent time points of adjacent trajectories. The density ratio is the inverse of the area ratio.

Figure 4.   Electrostatic potential contours for the zero bias potential case at zero transverse ion temperature. Contour levels are at intervals of half the electron temperature. The same plot for finite ion temperature is indistinguishable from this one.

Figure 5.   Electrostatic potentials contours for bias potential of -10θ at finite (300K) transverse ion temperature. Contour levels are at intervals of the electron temperature. The same plot for zero ion temperature is indistinguishable from this one.

Figure 6.   Ion density profiles for zero ion temperature calculated 15 Debye lengths downstream of the plate. The two curves are for plate bias potentials of zero (showing a peak and sharp drop at -0.5 Debye lengths) and -10θ (showing a sharp drop at -2.3 Debye lengths).

Figure 7.   Ion density profiles for finite (300K) ion temperature calculated 15 Debye lengths downstream of the plate. The two curves are for plate bias potentials of zero (showing a broadened front from +0.1 to -1.3 Debye lengths) and -10θ (showing a broadened front from -1 to -3 Debye lengths).

Figure 8.   Ion densities for

    (a) zero temperature, zero bias;

    (b) finite (300K) temperature, zero bias;

    (c) zero temperature, -10θ bias;

    (d) finite (300K) temperature, -10θ bias.

The spacing between contour levels is approximately 0.06, with several contour lines on the discontinuity ((a) and (c)) or in the shaded region ((b) and (d)).

Figure 9.   Measured ion density profile for -3V bias, together with the calculated curve for 300K ion temperature and -10θ bias.
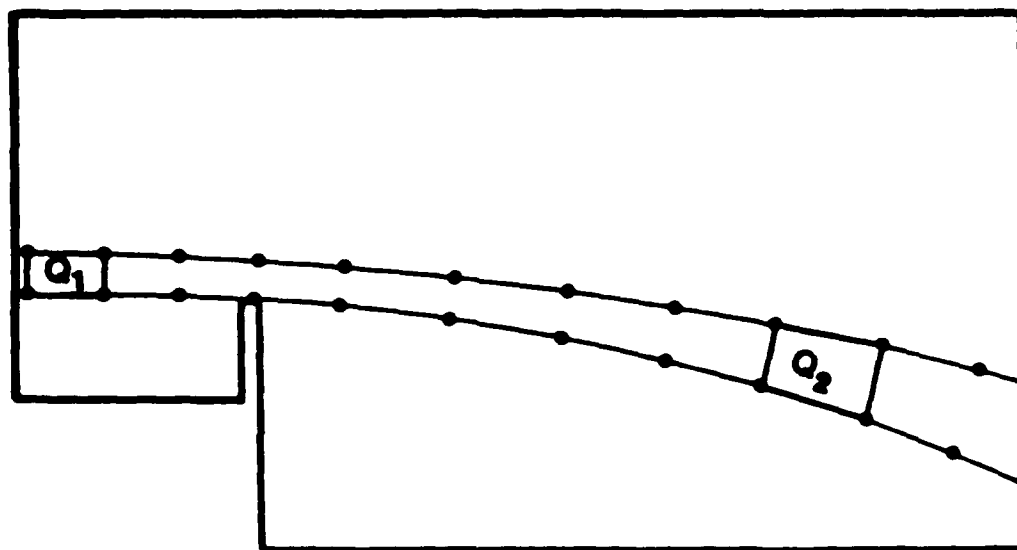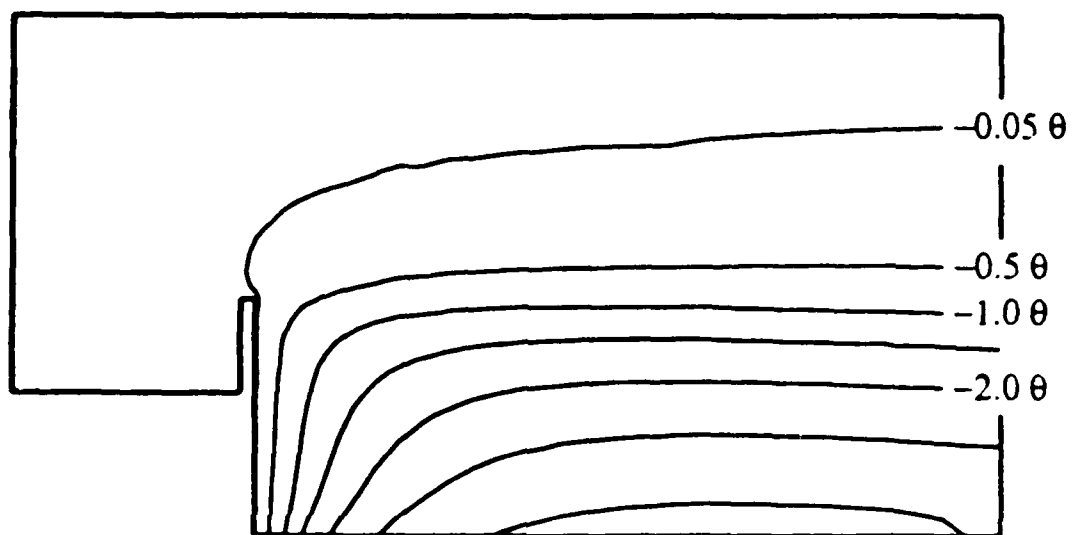
16

Figure 1

Figure 2

18

Figure 3

19

Figure 4

-0.1 θ

-1.0 θ

-2.0 θ

-5.0 θ
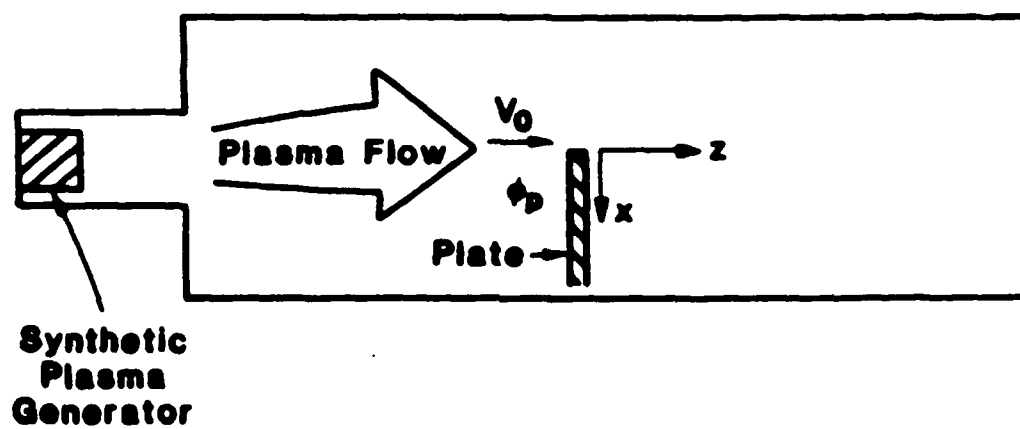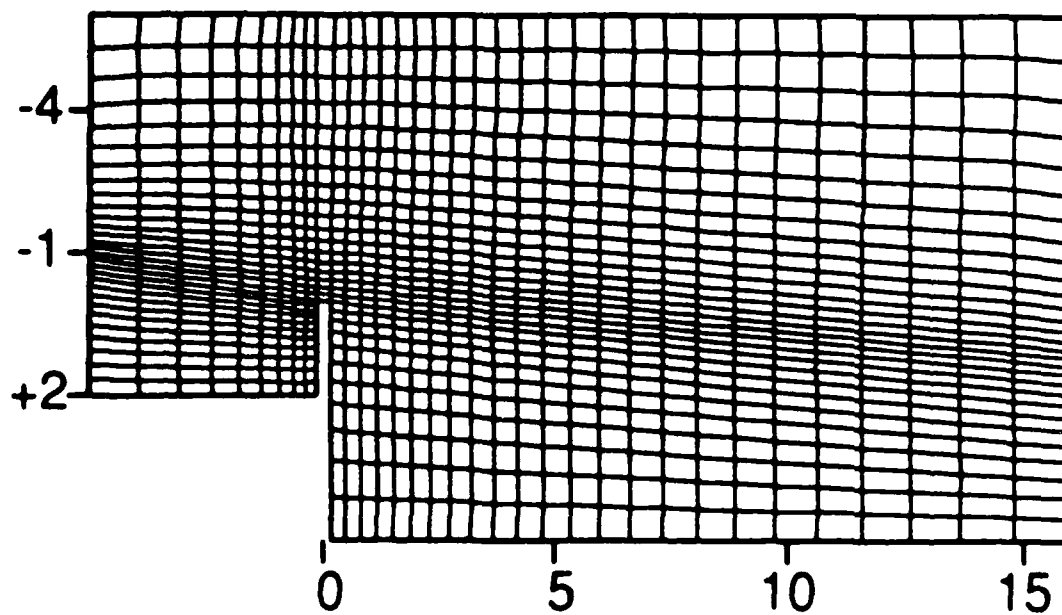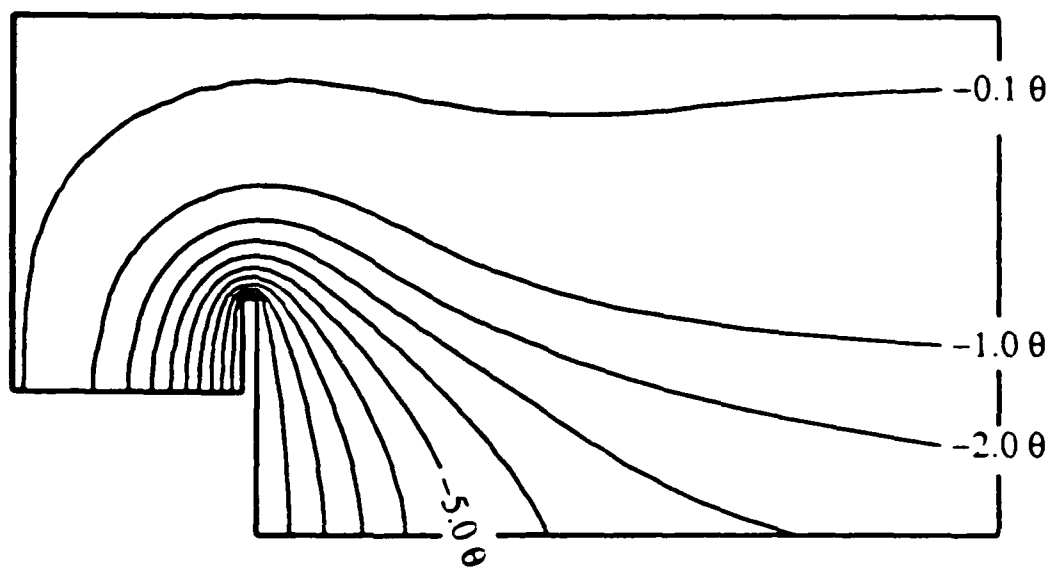
Figure 5

Zero Ion Temperature
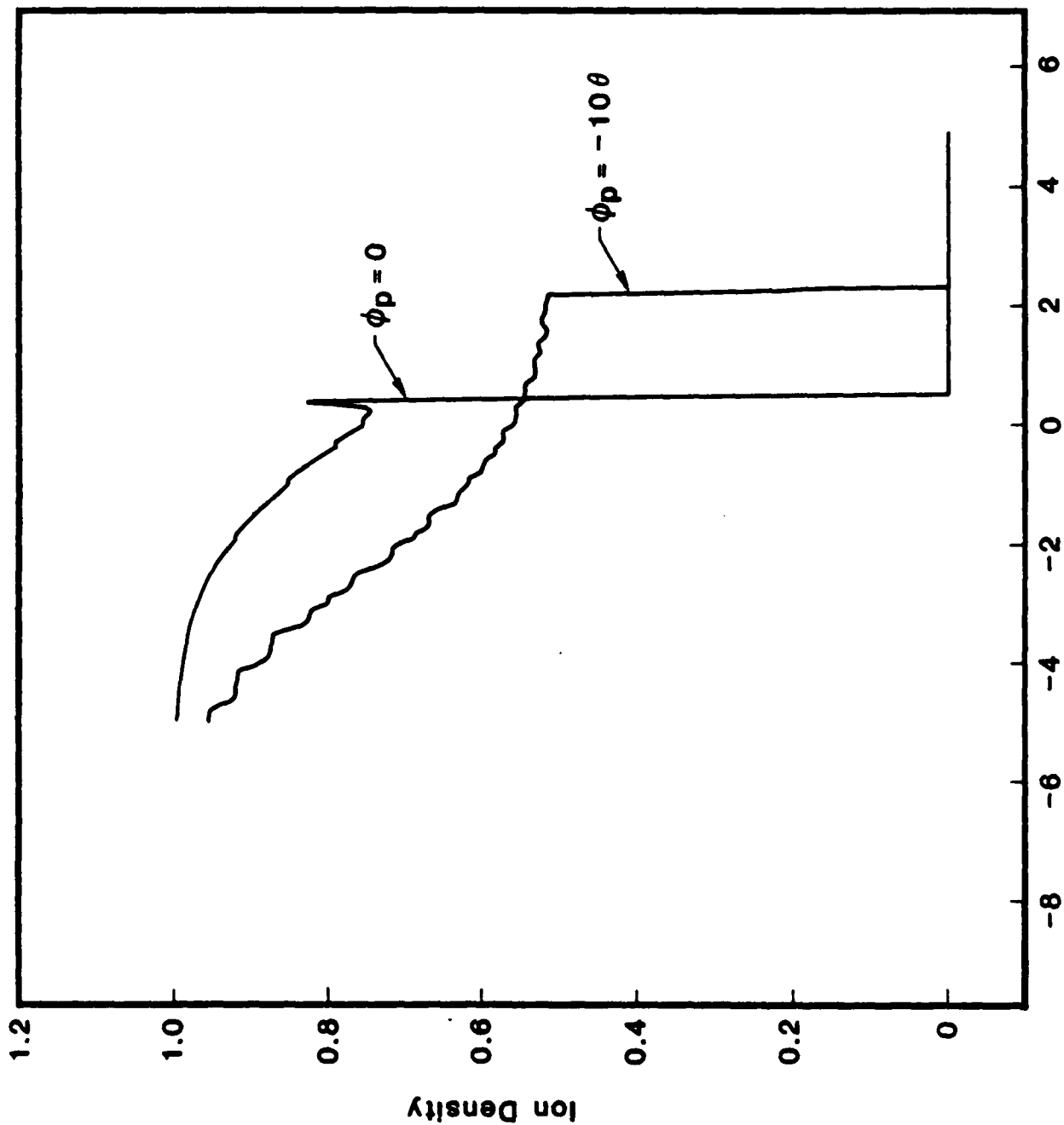
Transverse Position (λ_D)

Figure 6

$\phi_p = 0$

$\phi_p = -10\theta$

Ion Density

22

Finite Ion Temperature

$\phi_p = 0$

$\phi_p = -10\theta$

Ion Density

Transverse Position (λ_D)

Figure 7

23

$$\frac{n_i}{N} > 0.95$$

0.92 0.85 0.80

$$\frac{n_i}{N} < 0.05$$

(a)

Figure 8a

$$\frac{n_i}{N} > 0.95$$

0.80

0.92

0.85

$$\frac{n_i}{N} < 0.05$$

0.10

(b)

Figure 8b

Figure 8c

26

$\frac{n_i}{N} > 0.95$

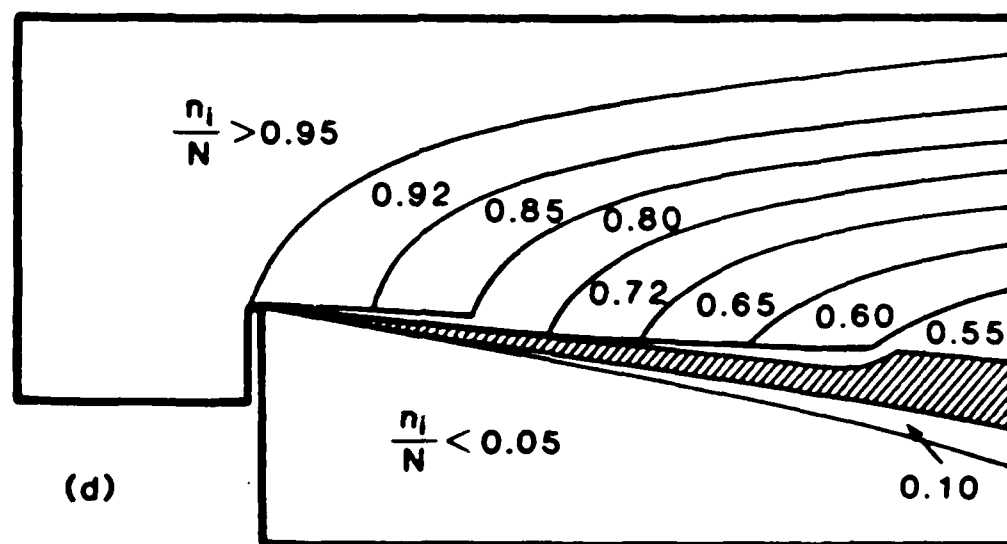0.92 0.85 0.80

0.72 0.65 0.60 0.55

$\frac{n_i}{N} < 0.05$

(d)

0.10
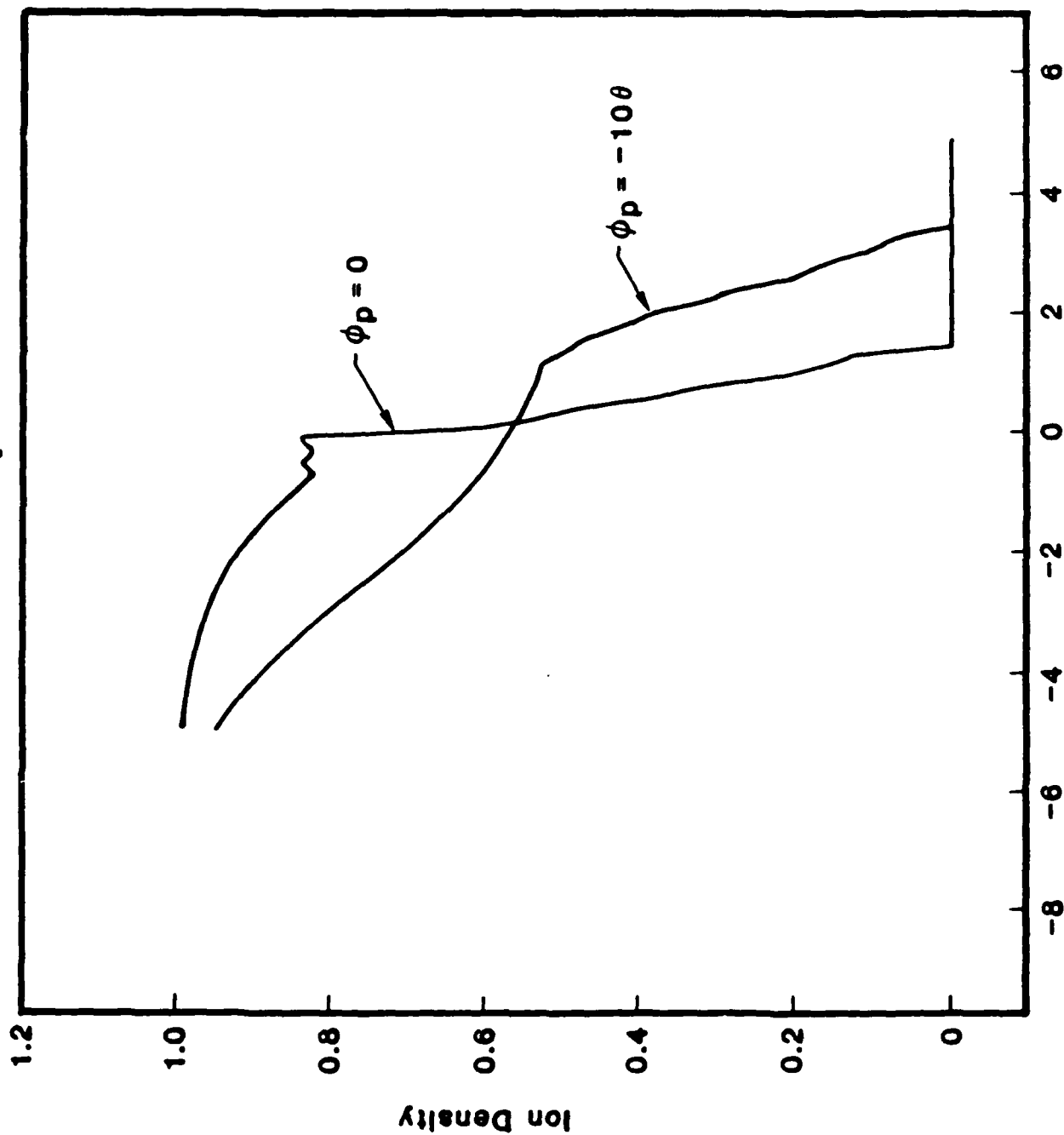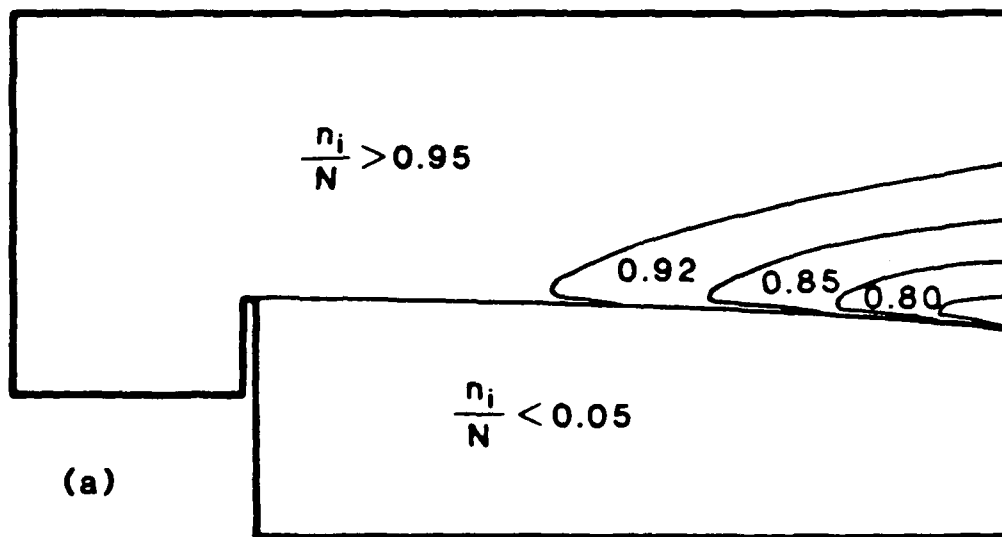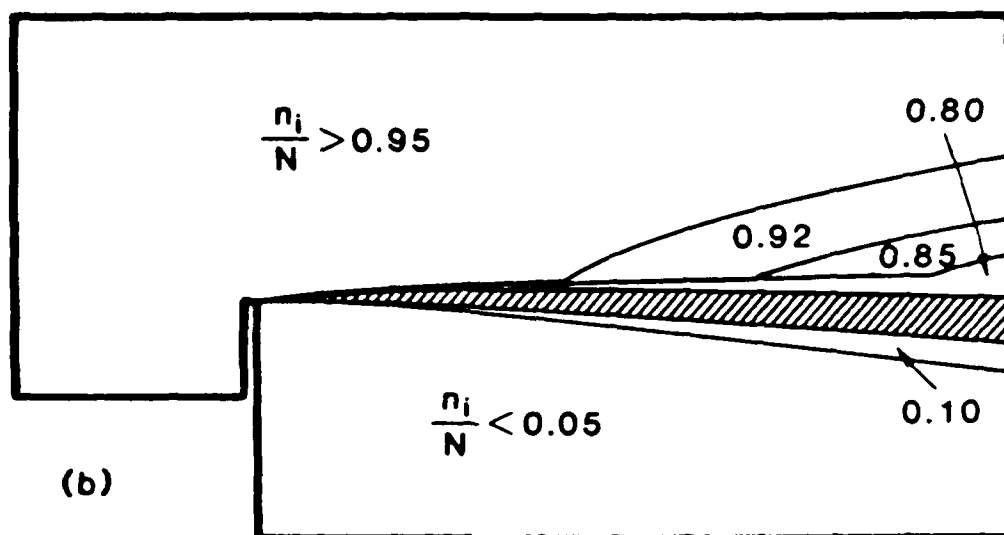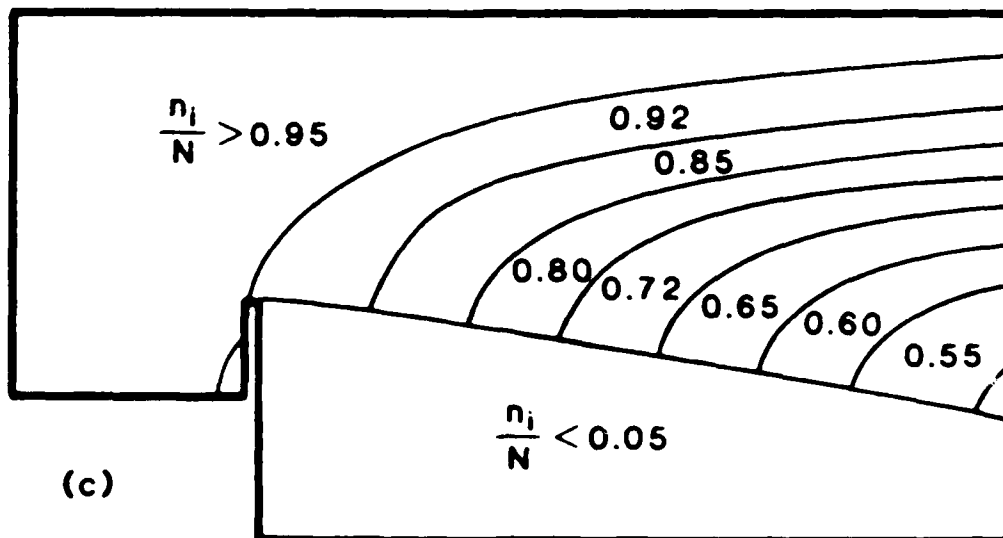
Figure 8d

Calculation vs. Experiment

Figure 9

28

END
10-81
DTIC